

On the numerical calculation of collapse and collapse propagation pressure of steel deep-water pipelines under external pressure and bending: Experimental verification of the finite element results

Rita G. Toscano, Luciano Mantovano and Eduardo N. Dvorkin^ξ

*Center for Industrial Research
TENARIS GROUP
Dr. Simini 250
2804 Campana, Argentina*

Keywords: collapse, finite element models, full scale testing

1. Introduction

In the design of marine pipelines it is fundamental to be able to determine the collapse pressure of steel pipes subjected to external hydrostatic pressure and bending and it is required to be able to quantify the effect of manufacturing imperfections such as ovality, eccentricity and residual stresses on the collapse pressure.

The tracking of the post-collapse equilibrium path is also necessary in order to assess on the stability of the post-collapse regime; that is to say, in order to assess if a collapse will be localized in a section or will propagate along the pipeline. Hence, it is also required to be able to analyze the effect of the geometrical imperfections and of the residual stresses on the collapse propagation pressure, which is the lowest external pressure that will propagate the collapse along the pipeline, for a constant applied curvature.

The finite element method is an adequate and reliable tool for the above mentioned studies [1-7].

Our purpose in this paper is to perform a verification of the finite element models; therefore, we compare finite element results and experimental results for full-scale collapse tests under external pressure, external pressure followed by bending and bending followed by external pressure.

The test program was performed at C-FER Technologies (C-FER), in Canada, using TENARIS steel seamless pipes [3]; while the finite element analyses were performed by CINI, in Argentina, using the general-purpose finite element code ADINA [8]. The numerical / experimental comparisons reported in this paper demonstrate a very good agreement between the finite element predictions and the laboratory observations.

2. The experimental program

The testing involved performing material property tests, initial geometry measurements, full-scale P tests (collapse and post-collapse under external pressure only), full-scale $P \rightarrow B$ tests (external pressure first, then increase bending up to collapse), and a full-scale $B \rightarrow P$ test (bending first, then increase external pressure up to collapse) on steel seamless pipe samples.

Nine samples were tested, all of them conforming to API 5L grade X65. The nominal dimensions for each sample are indicated in Table 1.

^ξ E-mail: dvk@siderca.com

Table 1. Tested samples

Sample	Nominal OD [mm]	Nominal wall thickness [mm]	Test
1	353	22	P
2	353	22	$P \rightarrow B$
3	353	22	$P \rightarrow B$
4	323.85	17.65	P
5	323.85	17.65	$P \rightarrow B$
6	323.85	17.65	$P \rightarrow B$
7	323.85	20.30	P
8	323.85	20.30	$P \rightarrow B$
9	323.85	20.30	$B \rightarrow P$

2.1. Geometrical characterization of the specimens

Geometric measurements were performed at CINI using:

- Manual ultrasonic gages for mapping the wall thickness at a number of points evenly distributed on the sample external surfaces.
- The *shapemeter*, described in Ref. [7], for acquiring a detailed description of the pipes OD.

Using the shapemeter a “best fit circle” is determined for transversal sections closely spaced (approx. 2 mm apart) and for each section the deviations between the actual radius at each point and the section “best fit radius” are plotted as a function of the polar angle: $f(\vartheta)$. A Fourier decomposition of $f(\vartheta)$ is then performed [7].

In Fig. 1, we show a photograph of the shapemeter and a detail of the $f(\vartheta)$ Fourier decomposition. In Fig. 2 we present a typical thickness distribution.

Here it is important to introduce some remarks:

- The imperfection mode that controls the value of the buckling pressure is the second one [7].
- The angular orientation of the second mode at each section has an important influence on the collapse pressure. When the ellipse that characterizes the second mode is rotated from one section to the next one, the collapse pressure is higher than for the case of aligned ellipses [7].
- The value of that second mode is quite different (lower) from the ovality measured with a standard API ovalimeter [9].

2.2. Mechanical characterization of the specimens

On longitudinal and circumferential coupons, the yield stress and hardening properties of the specimens steel were determined.

Using the standard ring-splitting test [7] the sample hoop residual stresses were determined.

2.3. Full-scale tests

C-FER Deepwater Experimental Chamber was used for all the full-scale tests. The chamber, shown in Fig. 3, has a tested pressure capacity of 62 MPa, with an inside diameter of 1.22 m and an overall inside length of 10.3 m.

Three collapse and buckle propagation tests were conducted. Two of the collapse tests required pressures in excess of 62 MPa. To achieve higher pressures, a secondary pressure vessel was used inside of the Deepwater Experimental Chamber, allowing pressures up to 80 MPa. Fig. 4 illustrates this arrangement. After initial collapse, continuing to pump water into the pressure vessel propagated the buckle.

In Fig. 5 we present the experimental set-up developed by C-FER for the cases that include bending.

A detailed description of the experimental procedures was presented in Ref. [3].

3. The Finite Element Analysis

In previous publications CINI presented finite element models that simulate the collapse and post-collapse behavior of steel pipes under external pressure and bending. Those finite element models were used to analyze the effect of different imperfections on the collapse pressure and on the collapse propagation pressure of the steel pipes [1-7].

The finite element models were developed using a material and geometrical nonlinear formulation [10] and they incorporate the following features:

- Geometry as described by the OD mapping and by the thickness distribution measured as reported above.
- MITC4 shell element [11-13].
- Von Mises elastic - perfectly plastic material model with the yield stress corresponding to the samples hoop yield stress in compression. In this model the plastic anisotropy of the material is neglected.
- Circumferential residual stresses as reported above.
- Contact elements on the pipe inner surface [10] in order to prevent its inter-penetration in the post-collapse regime.
- Nonlinear equilibrium path tracking via the algorithm described in Ref. [14].

In what follows, in order to validate the numerical models, for the nine tests described in Table 1 we compare the finite element results with the full-scale test results.

3.1. P- Tests

In Fig. 6, for the pipes under external pressure only, the experimentally and numerically determined [*External Pressure vs. Internal Volume Reduction*] diagrams are compared.

In the three cases both diagrams are practically coincident, except in the interval that goes from immediately after the pipe collapse to the point at which the experimentally and numerically determined curves merge again. In the experimental test, after collapse the chamber is abruptly depressurized and water must be pumped to regain pressure. Hence, the [*External Pressure vs. Internal Volume Reduction*] experimental path is different from the numerical one, which better represents the undersea conditions.

From the presented results we can assess that the post-collapse response of the finite element model, specifically the path in which the collapse propagates, has an excellent match with the experimental results.

The raising part of the collapse pressure in the post-collapse regime is due to the contact between points on the pipe inner surface (e.g. in the first sample the pressure raises from $1kg/mm^2$ to approximately $1.22kg/mm^2$ which is the pipe propagation pressure)

For one of the samples, in Figs. 7 and 8, we show the deformed mesh in the post-collapse regime. However, to achieve the matching between the finite element predicted collapse modes and the laboratory observed ones it is required the further refinement of the analysis techniques, taking into account the presence of multiple collapse modes for the same collapse load.

In the following table we summarize the results of a sensitivity analyses numerically performed for the external collapse pressure:

Table 2. Sensitivity analyses for the P-tests

Sample	pc FEA / pc exp Sample 1	pc FEA / pc exp Sample 4	pc FEA / pc exp Sample 7
Baseline ¹	0.977	0.966	1.103
Min. Axial Res. Stresses ²	0.983	1.004	1.124
Max. Axial Res. Stresses ³	0.971	0.917	1.081
Min. Hoop Res. Stresses ⁴	0.979	0.982	1.11
Max. Hoop Res. Stresses ⁵	0.975	0.948	1.096
Min. Yield Stress ⁶	0.889	0.872	0.998
Max. Yield Stress ⁷	1.062	1.058	1.207

It is clear that the largest influence on the external collapse pressure comes from the material yield stress. However, as already discussed in Refs. [1, 3], the influence of the material yield stress on the collapse propagation pressure is quite low. With the developed finite element model we get,

¹ In this case the results were obtained using the measured data with no axial residual stresses

² Equal to – (measured hoop residual stresses)

³ Equal to (measured hoop residual stresses)

⁴ 0.9*baseline residual stresses

⁵ 1.1*baseline residual stresses

⁶ 0.9*baseline yield stress

⁷ 1.1*baseline yield stress

$$\frac{\partial p_{col}}{\partial \sigma_y^o} = 0.100$$

$$\frac{\partial p_{prop}}{\partial \sigma_y^o} = 0.013$$

3.2. P→B Tests

In this cases the 5 samples were first loaded with external pressure and afterwards, maintaining constant the external pressure, they were bent up to collapse.

In the following table we summarize the comparison between the numerical and experimental results:

Table 3. Results for pressure plus bending

Sample	$\frac{\text{Applied External pressure}}{\text{DNV collapse pressure}}^8$	Collapse moment: $\frac{\text{Numerical}}{\text{Experimental}}$
2	0.822	1.047
3	0.735	1.088
5	0.541	0.972
6	0.881	0.998
8	0.823	0.998

3.3. B→P Tests

The ninth sample was bent up to a maximum bending strain of 1.33% and afterwards, maintaining the bending strains constant, it was loaded with an increasing external pressure up to collapse.

$$\frac{\text{Numerical collapse pressure}}{\text{Experimental collapse pressure}} = 0.964$$

In Figs. 9 and 10 we compare the numerically and experimentally determined transversal sections at collapse.

4. Conclusions

The agreement between the finite element predictions and the laboratory observations is excellent; hence, the developed finite element models can be used as reliable engineering tools for assessing on the collapse and post-collapse behavior of tubular products.

⁸ DNV-collapse pressure was determined using this standard [15] for the case of external pressure only.

5. References

1. R.G.Toscano, M.Gonzalez and E.N.Dvorkin, "Validation of a finite element model that simulates the behavior of steel pipes under external pressure", *The Journal of Pipeline Integrity*, **2**, pp.74-84, 2003.
2. R.G.Toscano, M.Gonzalez and E.N.Dvorkin, "Experimental validation of a finite element model that simulates the collapse and post-collapse behavior of steel pipes", *Proceedings Second MIT Conference on Computational Fluid and Solid Mechanics*, (Ed. K.-J. Bathe), Elsevier, 2003.
3. R.G.Toscano, C.Timms, E.N.Dvorkin and D.DeGeer, "Determination of the collapse and propagation pressure of ultra-deepwater pipelines", *Proceedings OMAE 2003 - 22nd. International Conference on Offshore Mechanics and Arctic Engineering*, 2003.
4. R.G.Toscano and E.N.Dvorkin, "Collapse and post-collapse behavior of steel pipes", *Proceedings Fifth World Congress on Computational Mechanics*, Vienna, Austria, 2002.
5. R.G.Toscano, P.M.Amenta and E.N.Dvorkin, "Enhancement of the collapse resistance of tubular products for deep-water pipeline applications", *Proceedings 25th. Offshore Pipeline Technology Conference*, IBC, Amsterdam, 2002.
6. E.N.Dvorkin and R.G.Toscano, "Effects of external/internal pressure on the global buckling of pipelines", *Proceedings First MIT Conference on Computational Fluid and Solid Mechanics*, (Ed. K.-J.Bathe), Elsevier, 2001.
7. A.P.Assanelli, R.G.Toscano, D.H.Johnson and E.N.Dvorkin, "Experimental / numerical analysis of the collapse behavior of steel pipes", *Engng. Computations*, **17**, pp.459-486, 2000.
8. The ADINA System, ADINA R&D, Watertown, MA, USA.
9. A.P. Assanelli and G. López Turconi, "Effect of measurement procedures on estimating geometrical parameters of pipes", *2001 Offshore Technology Conference*, Paper OTC 13051, Houston, Texas, 2001.
10. K.J. Bathe, *Finite Element Procedures*, Prentice Hall, NJ, 1996.
11. E.N.Dvorkin and K.J.Bathe, "A continuum mechanics based four-node shell element for general nonlinear analysis", *Engng. Computations*, **1**, pp. 77-88, 1984.
12. K.J.Bathe and E.N.Dvorkin, "A four-node plate bending element based on Mindlin / Reissner plate theory and a mixed interpolation", *Int. J. Numerical Methods in Engng*, **21**, pp. 367-383, 1985.
13. K.J.Bathe and E.N.Dvorkin, "A formulation of general shell elements - the use of mixed interpolation of tensorial components", *Int. J. Numerical Methods in Engng*, **22**, pp.697-722, 1986.
14. K.J.Bathe and E.N.Dvorkin, "On the automatic solution of nonlinear finite element equations", *Computers & Structures*, **17**, pp. 871-879, 1983.
15. Offshore Standard DNV-OS-F101 Submarine Pipeline Systems, 2000

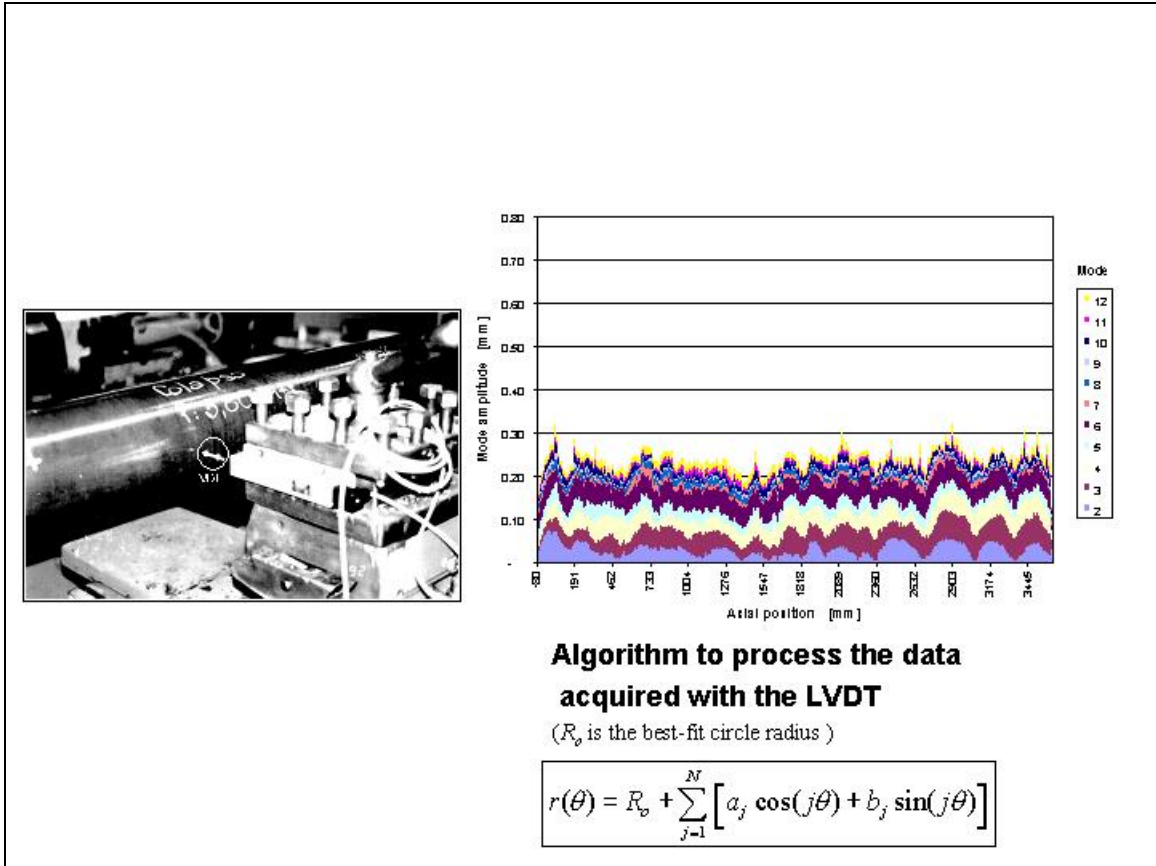


Figure 1. The shapemeter

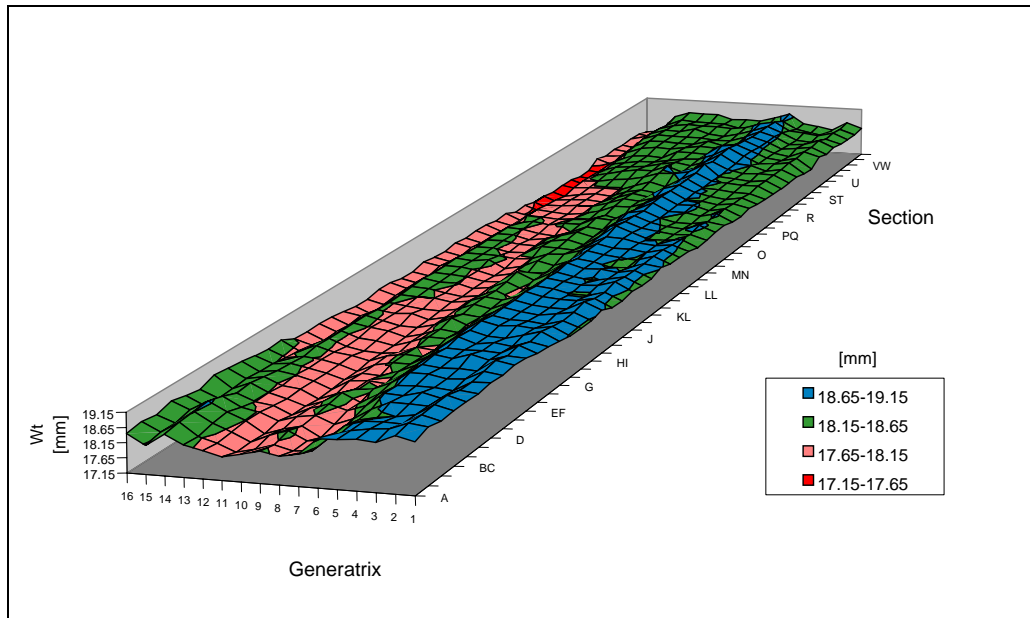


Figure 2. Typical thickness distribution



Figure 3. C-FER Deepwater Collapse Chamber

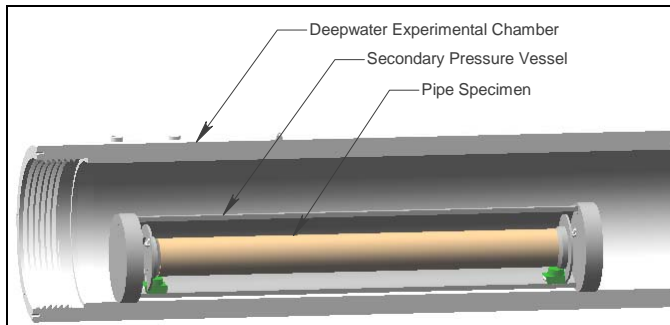


Figure 4. Pipe-in-pipe set-up for high-pressure tests

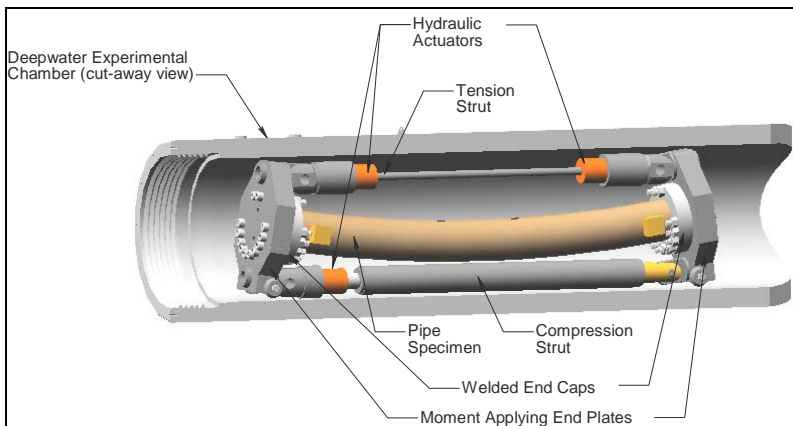


Figure 5. Experimental set-up for the cases that include bending

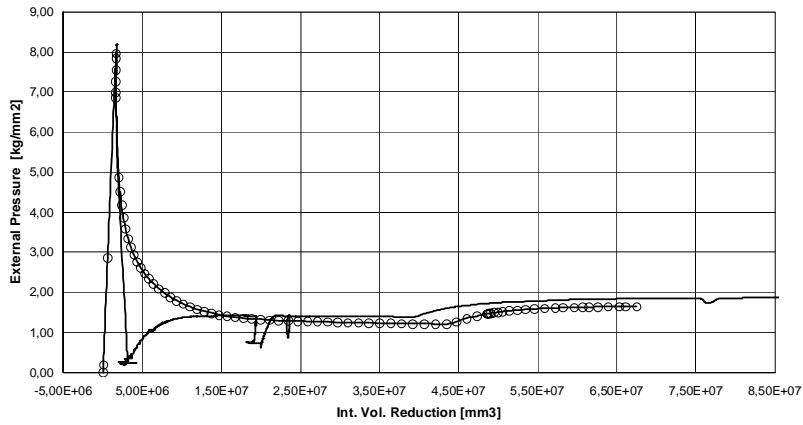
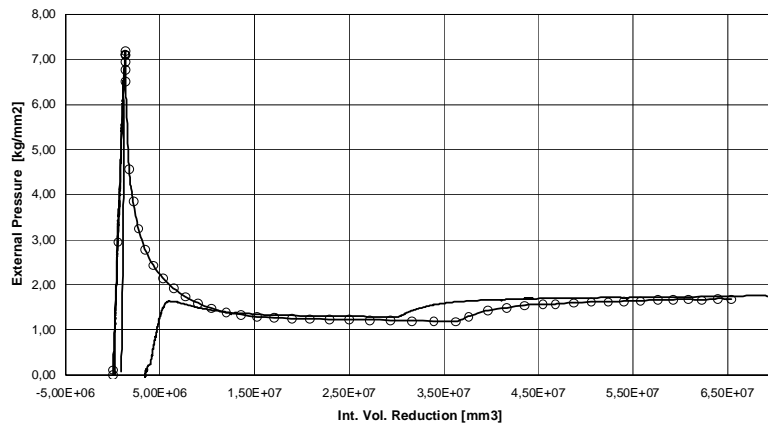
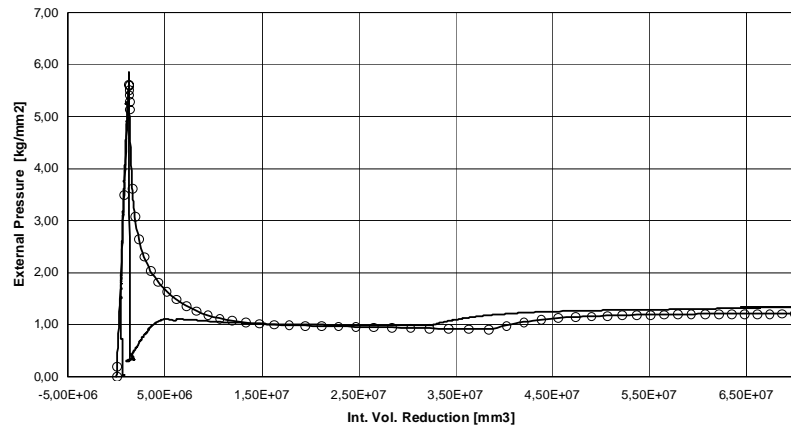


Figure 6. Tests 1, 4 and 7 external pressure vs. internal volume reduction; finite element curve (line and symbols) and experimental results (solid line)

